Characterization and Stability of Heteropolyacid Catalysts Supported on MCM-41 Materials Synthesized by Ultrasonic Irradiation

SONG IL KONG[1,2], DANUTA MATEI[2], DIANA CURSARU[2], VASILE MATEI[2], DRAGOS CIUPARU[2]*

[1] Petroleum - Gas University of Ploiesti, Department of Petroleum Processing Engineering and Environmental Protection, 39 Bucharest Blvd, 100680, Ploiesti, Romania

[2] Department of Chemistry, Kim Il Sung University, Str. Kumsong, Pyongyang, D. P. R. of Korea

A series of solid acid catalyst of the Keggin-type 12-phosphotungstic acid, $H_3PW_{12}O_{40}$, supported on ordered mesoporous silica MCM-41 were prepared by a simple and effective impregnation method. MCM-41 supports were synthesized in a relatively short time via a recently reported ultrasonic irradiation method. The synthesis sonication time has been systematically varied in order to investigate its influence on the structural order of the resulting materials. The prepared catalysts were characterized by nitrogen adsorption, X-ray diffraction, Raman spectroscopy and thermogravimetric analysis. The resulting materials exhibited hexagonally ordered meso structure, with high surface area of the order of several hundreds of m^2g^{-1},relatively large pore volumes, with the pore diameter in the range of 2.19 to 2.41 nm and a corresponding pore wall thickness of over 1.67nm. The results have demonstrated that high quality MCM-41 materials can be synthesized via the ultrasonic irradiation in few tens of minutes, much shorter than the conventional synthesis methods. Despite their relatively high loading, all synthesized materials retained the characteristic MCM-41mesoporous structure after impregnation of the heteropolyacid active phase onto the inner pore surface, without crystallization, but preserving the Keggin structure as confirmed by Raman spectroscopy.

Keywords: MCM-41, Ultrasonic irradiation, Heteropolyacid, HPW/MCM-41, Catalyst stability

Heteropolyacids are suitable acid catalysts for a wide variety of reactions in homogeneous phase offering a convenient alternative for efficient and cleaner processes when compared to the conventional mineral acids [1,2]. In particular, heteropolyacids (HPAs), such as 12-tungstophosphoric acid ($H_3PW_{12}O_{40}$, HPW) and 12-tungstosilicic acid ($H_4SiW_{12}O_{40}$, STA) have attracted much attention because of their stable and strong acidity, high oxidation potential and redox characteristics, which enables these materials to play both as Brønsted acid and redox catalysts [2-5]. However, HPAs suffer from two major drawbacks, namely, (i) very low surface area (< 10 m^2g^{-1}) in the solid phase, and (ii) high solubility in polar solvents. These problems may be overcome by immobilizing HPAs on high surface area supports like silica, zeolites, or mesoporous materials [6].

Since the discovery of ordered mesoporous materials in the early 1990s [6, 7], the MCM-41 materials have attracted considerable interest because of their high surface area, regular pore structure, specific pore volume and high thermal stability. Compared to zeolites, the regular structure of MCM-41materialsis amorphous, and all their characteristics make them suitable for many catalytic applications [8, 9].The mesoporous materials are usually prepared by the hydrothermal method, which requires high temperatures and long periods of time [10], which severely hampers their practical applications. For many applications, such as adsorbent or catalytic materials, it would be desirable to have more feasible methods to prepare silica MCM-41 in a shorter synthesis time. So far, MCM-41 materials prepared via the original hydrothermal method have been widely investigated [11-15], while synthetic routes for MCM-41 materials involving less time consuming processes have been rarely reported in comparison to the vast literature published for the classical hydrothermal method.

Various methods had been explored for the synthesis of ordered mesoporous silica in shorter synthesis time, with preserving the good quality of the resulting materials [16,17]. In this respect, the sol-gel method is considered to be an effective method for the synthesis of silica MCM-41that offers the advantage of reducing the crystallization time compared to the conventional method. For example, Voegtlin et al. [18] have prepared highly ordered MCM-41 at room temperature in one hour. However, the stability of the material above 600°C was lost. Melendez-Ortiz et al. [19] have synthesized MCM-41 at room temperature for 3h and obtained stable materials via this fast and reproducible method, without adding any additives. However, silica MCM-41 materials prepared by sol-gel condensation have some drawbacks as they require longer aging time and result in smaller surface area [20]. In contrast to these reports on room temperature syntheses that do not require specialized equipment, the method involving microwave irradiation offers the advantage of a reduced crystallization time [21], although, most likely, it does not seem suitable for industrial scale production.

Recently, ultrasonic irradiation has been introduced for the synthesis of materials with unusual properties [22–24]. To reduce the synthesis time for economic benefits, the use of ultrasound irradiation is now a subject of growing interest for the preparation of a variety of nanostructured materials, due to the special acoustic cavitation effect [25], which creates special stirring conditions, high local temperatures and high pressures in liquids and, eventually, it can increase the rates of chemical reactions. Hanu et al. [26] have investigated the effects of ultrasonic irradiation on the MCM-41 synthesis in acidic and basic conditions. The synthesis time of MCM-41materials was shortened to 1h, but the specific surface area of the resulting material was 731m^2g^{-1} in basic environment, a lower value compared to 1320 m^2g^{-1} in acid conditions. The *p*H of the synthesis solution has been previously observed to influence the physicochemical properties of MCM-41 materials [27]. Tang et al. [20] also reported the synthesis of mesoporous silica MCM-41 with hexagonal arrangement

* email: dciuparu@upg-ploiesti.ro Phone: + 40 - 244.573 171

and narrow distribution of mesopore diameters via ultrasonic irradiation under basic environment; however, in synthesis they used sonication for 3.5hours, followed by aging, with and without heating, for 28h. The thickness of pore walls in their resulting materials was improved, but the specific surface area was modest: $835 m^2g^{-1}$ and $931 m^2g^{-1}$. Run et al. [28] reported the synthesis of mesoporous molecular sieves with specific surface areas as high as $1100\ m^2g^{-1}$, similar to MCM-41 obtained under acidic conditions, by ultrasonic irradiation for a short time of about 20 minutes, but after aging for 5 hours. Recently, Vetrivel el al. [29] reported the preparation of MCM-41 at room temperature after ultrasonic irradiation for 5 minutes. So far, this is the shortest synthesis time for MCM-41 materials and the resulting specific surface area is the largest, but the stability has not been characterized and the structure might hold to lower temperatures than that obtained by the conventional method due to a thinner estimated wall thickness of only 1.24 nm.

The use of ultrasonication has been extended to the synthesis of other mesoporous molecular sieves as well. Recently, Palani et al. achieved the synthesis of SBA-15 by a temperature-assisted ultrasonic method [30]. Lee et al. [31] also reported the synthesis of SBA-15 and Ti-SBA-15 molecular sieves with ultrasonic irradiation for 1 h, followed by gelation for 1–3 h.

The main advantage of the ultrasonic technique for the synthesis of mesoporous materials is the important reduction of the preparation time from 1 to 3 days to few or several hours. Moreover, the mesoporous materials obtained by ultrasonic irradiation have better thermal stability than the corresponding sol–gel materials [20], which is attributed to the thicker walls of the mesoporous silica obtained by ultrasonic synthesis [22]. However, to the best of our knowledge, there are no reports of a systematic investigation of the influence of the sonication time on the characteristics of the resulting materials. Thus, the purpose of this work was to prepare highly ordered and thermally stable mesoporous MCM-41 materials under basic environment via ultrasonic irradiation, and to systematically investigate the effects of the synthesis sonication time on the structure and properties of the resulting materials. We have further used the synthesized mesoporous molecular sieves as supports to immobilize HPW for catalysis purposes.

Experimental part

Materials

All chemicals, tetraethyl orthosilicate, TEOS (98%), cetyltrimethyl-ammonuim bromide (CTABr, 98%), 12-tungstophosphoric acid ($H_3PW_{12}O_{40} \cdot xH_2O$), ammonia solution (15.3 mol/L), ethanol (EtOH, 99.8 wt%), methanol (MtOH, 99.8 wt%)used for the synthesis of mesoporous molecular sieve supports and the HPW/MCM-41 catalysts were purchased from Sigma Aldrich. These chemicals were used without further purification.

Synthesis of MCM-41materials

MCM-41materials were prepared following two steps. The synthesis initially followed the procedure described in the literature [30]. In a typical synthesis, 1.555g (0.00426 mol) of cetyltrimethyl-ammonium bromide, CTMABr was dissolved in 12mL (0.1839 mol) ammonia solution diluted with 50mL of distilled water under stirring at room temperature to obtain a homogeneous solution. After complete dissolution, 12mL (0.2058 mol) of ethanol were added to the solution. Subsequently, 3.111 g (0.0149 mol) of TEOS were added drop wise into the solution under vigorous stirring.

The resulting solution was subjected to sonication using an ultrasonic generator (Sonicator HD 2200; Bandeline, MS 72, Germany), equipped with a converter/transducer and titanium oscillator (horn), 13 mm in diameter, operating at 20 kHz with a maximum power output of 200W for the desired time ranging from 15 to 60min, i.e. 15, 30 and 60 min. The ultrasonic generator automatically adjusts the power level. The wave amplitude in each experiment was adjusted accordingly. The molar composition of the reaction mixture was 1TEOS: 0.286 CTMABr: 13.8 EtOH: 12.3 NH_3. The resulting precipitate was filtered, washed with demineralized water to *p*H=7, dried in an oven at 80°Covernightand then calcined in argon flow while heating at 3 °C min^{-1} from room temperature to 550 °C, then soaked at 550°C for 6 h in order to remove the surfactant. The resulting samples are denoted as MCM-41(x), where x represents the sonication time in minutes.

Preparation of HPW/MCM-41 catalysts

The HPW was supported on MCM-41 by the impregnation method. One gram of calcined MCM-41 was dispersed under stirring into a solution of the desired amount of HPW in 20 mL of methanol for 3h. After removing the methanol by evaporation, the sample was dried at 110 °C overnight in oven and subsequently calcined at 285 °C for 3h in air.

Characterization

A detailed physical and chemical characterization of the carriers and supported HPW was carried out by using different techniques: namely, nitrogen adsorption–desorption isotherms, X-ray diffraction (XRD), Raman spectroscopy and DTG.

X-ray diffraction (XRD) patterns of samples were determined using a D8 ADVANCE Nova diffractometer. The patterns were obtained with copper radiation (Cu K_α, λ=1.5406Å) with the second monochromator at 40kV and 40 mA, at a scanning speed of 2° in 2θ/min. The samples were scanned from 1 to 70° (2θ) angle in steps of 0.02°, with a count of 5s at each point. Thermogravimetric analysis (TG/DTG) of samples was performed using a Setaram Instrument LABSYS evo, which operates in the temperature interval from room temperature to 800°C, under flowing argon, at a heating rate of 5°C / min. The adsorption isotherms and the specific surface area (S_{BET}) of the various materials were determined from nitrogen adsorption isotherms collected at 77K using a Quantachrome Autosorb Automated Gas Sorption system. Before the measurement, each sample was degassed overnight at 573 K. Adsorbed nitrogen volumes were normalized to standard temperature and pressure. The Brunauer-Emmett-Teller (BET) method was used to calculate the multipoint BET surface area. The pore size distribution was derived from the desorption branches of the isotherms using the Barrett-Joyner-Halenda (BJH) method. The total pore volume, V_p, was estimated from the amount adsorbed at a relative pressure of p/p_0 = 0.99. The Raman spectra of the samples were recorded on a confocal microscope Renishaw Raman type in Via Raman microscope using a laser radiating at 633 nm and the 10x microscope objective.

Results and discussions

Nitrogen adsorption isotherms

The textural properties of the solids were measured by the N_2 adsorption–desorption isotherms method. The nitrogen adsorption–desorption isotherms of MCM-41(x), where x stands for the sonication time expressed in

Catalysts	$d^a_{(1\,0\,0)}$(nm)	a^b_0(nm)	S^c_{BET} (m^2g^{-1})	V^d_p(cm^3g^{-1})	D^e_p(nm)	δ^f (nm)
MCM-41(30)	3.53	4.08	1435	0.914	2.41	1.67
MCM-41(60)	3.27	3.78	1538	1.030	2.45	1.33
10%HPW/MCM-41	3.49	4.03	1352	0.843	2.36	1.67
20%HPW/MCM-41	3.46	3.99	860	0.610	2.31	1.68
30%HPW/MCM-41	3.53	4.08	460	0.208	2.19	1.89

[a] d-Spacing of (1 0 0) reflection.

[b] Unit cell constant, $a_0 = 2\,d_{100}/\sqrt{3}$

[c] BET surface area, calculated from the linear part of the BET plot.

[d] Total pore volume, taken from the volume of N_2 adsorbed at $P/P_0 = 0.99$.

[e] Average pore diameter, estimated using the desorption branch of the isotherm and the Barrett–Joyner–Halenda (BJH) formula.

[f] The pore wall thickness estimated from the difference $(a_0 - D_p)$.

Table1
TEXTURALPROPERTIESOFTHEHPW/ MCM-41 CATALYSTS

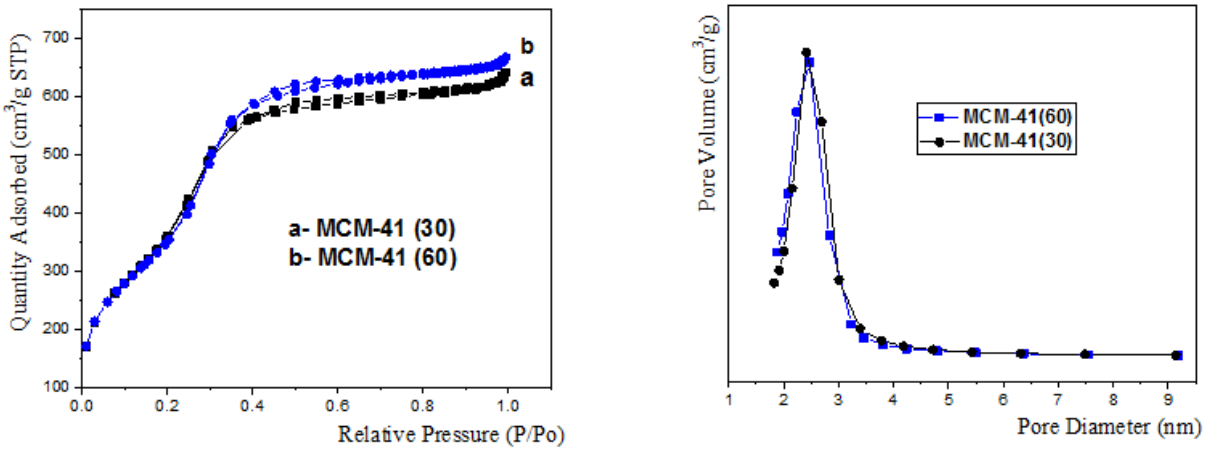

Fig.1. N_2 adsorption–desorption isotherms of calcined MCM-41 and pore size distribution, where (a) 30min, (b) 60min

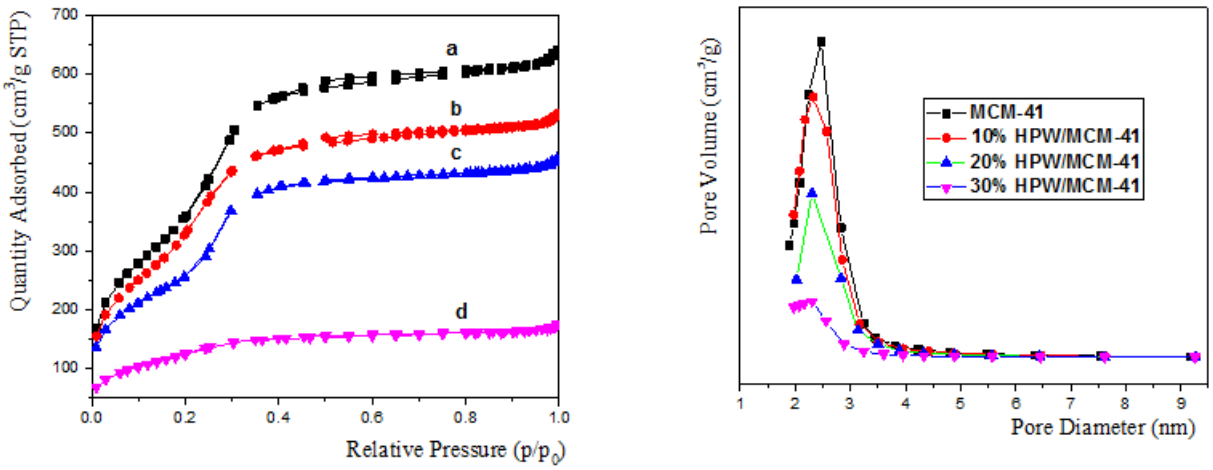

Fig.2. N_2 adsorption–desorption isotherms and pore size distribution of the catalysts: (a) MCM-41, (b) 10% HPW/MCM-41, (c) 20% HPW/MCM-41, and (d) 30% HPW/MCM-41

minutes, are shown, along with their pore size distributions, in figures 1 and 2. The corresponding structural properties of these samples, and those resulting after impregnation of HPW at different concentrations on MCM-41(30), depicted as y HPW/MCM-41 –where y stands for the HPW weight loading, are listed in table 1.

The isotherms for the MCM-41 samples are identified as type IV according to IUPAC nomenclature, indicating that the samples retain their hexagonal structure, preserving a relatively narrow pore size distribution after template removal. The BET surface areas and pore volumes of MCM-41(x) samples are in the range 1435–1538 m^2g^{-1} and 0.91–1.03 cm^3g^{-1}, respectively. The surface areas observed are significantly higher than those of conventional silica MCM-41. It has been reported that the ammonia-containing medium favors the formation of longer micelles [33]. This is likely the reason for the higher surface areas in the MCM-41(x) samples obtained by sonication compared to the sol-gel method. A rather small hysteresis was observed for the MCM-41(30) and MCM-41(60) samples, indicating the presence of porosity also formed from the agglomeration of silica nanoparticles. On the other hand, Vetrive et al. [29] have synthesized silica MCM-41 with the surface area over 1662 m^2g^{-1}, the pore volume over 0.89cm^3g^{-1}, the pore size over 2.6 nm and the wall thickness over 1.24nm after ultrasonic irradiation for 5 min. According to their experimental results the surface areas have noticeably decreased, but the pore volumes and the pore sizes were affected by the increase of the duration of ultrasonic irradiation. In particular, the textural stability is

increased when the time of the ultrasonic irradiation increased, but the wall thickness decreases below 1.22nm because the temperature of the sonication bath has risenafter 50 min, thus, it shows that relatively stable MCM-41 materials could be synthesized in the range of 20 min due to the larger resulting wall thickness. It is quite obvious that ultrasonic processing favors a thicker wall formation. Though acoustic cavitation etched the particles, resulting in a coarse outer surface, whereas the inside channels retained the hexagonal arrangement, the electron diffraction pattern shows higher order spots, which provide evidence that both the pore array and pore walls are highly ordered [29].

In our case, the synthesis time of the MCM-41(30) is relatively short; however, a highly ordered and stable mesostructure was obtained. It was previously reported that MCM-41 can be prepared in a few hours under ambient conditions, but few data regarding the stability of these materials had been presented [20, 34].The pore wall thickness of MCM-41(30)is larger than that of MCM-41(60). This is quite promising since high quality MCM-41 materials can be synthesized by a similar procedure, as well as in a shorter time than by the conventional method.

Table 1 lists the textural properties of pure MCM-41 and the supported HPW/MCM-41. These properties include d_{100} the d-spacing of the (100) diffraction in nm, a_0 (unit cell in nm), S_{BET} (BET surface area in m^2g^{-1}), pore volume in cm^3g^{-1}, and the average pore diameter in nm.

The HPW containing samples show a sharp inflection in the adsorption condensation region, at relative pressure $p/p_o = 0.2 - 0.4$. The BET surface area and the pore volume ofthe HPW/MCM-41 samples decreased from 1435 to $460 m^2g^{-1}$and from 0.914 to $0.208 m^3g^{-1}$, respectively, as the HPW loading increased from 0to 30% weight. However, the pore size distribution is centered from 2.19 to 2.41 nm, with larger pore diameters for lower HPW loading. In figure 3 we show the change in pore diameter and the pore volume as the HPW loading varies from 0 to 30% wt. It is evident that the pore volume and the specific surface area of the loaded sample are significantly lower compared to that of the pure MCM-41. The reduction in the pore volume and surface area after HPW loading is most likely due to the HPW deposited inside the channels as well-dispersed crystallites on the surface of the hexagonally ordered mesoporous MCM-41 support, consistent with the XRD results discussed below.

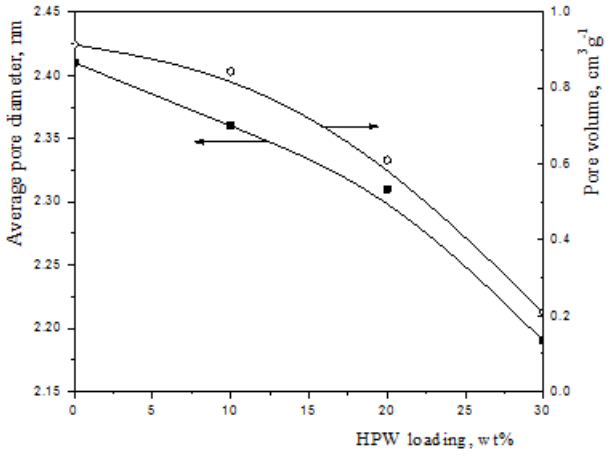

Fig. 3. Influence of HPW content in HPW/MCM-41 catalysts on the pore diameter and the pore volume

XRD

The powder X-ray diffraction (XRD) patterns of both, as-synthesized and calcined, samples (fig. 4) exhibited four diffraction peaks, associated to the (100), (110), (200) and (210) reflections of the closed packed hexagonal arrangement of the porous structure, in agreement with previous reports [6, 7]. We should mention that the sample prepared using sonication for 15 minutes did not show ordered mesoporous structure in XRD, nor the specific type IV nitrogen adsorption isotherm. As seen in figure 4, the sharp (100)peak appears at $2\theta < 3$, corresponding to interplanar spacing, $d_{100}$of 3.53 and 3.27 nm for sonication times corresponding to 30and 60min, respectively. Other two extremely weak peaks,(110) and (200), indexed to the hexagonal unit cell, are present between 2θ values of 3 and 6.The XRD peak positions of the as-synthesized materials shifted to lower 2θ values when the synthesis sonication time increased from 30 to 60 min. After calcination, the peaks shifted to higher 2θ values due to pore size contraction during the thermal treatment. The intensities of the diffraction peaks increase significantly after calcination, which is likely related to the removal of the occluding surfactant molecules during the calcination process, resulting in the enhancement of the long range structural ordering [35]. This result demonstrated that the formation of highly ordered mesoporous silica analogous to hexagonal silica MCM-41 could be achieved in as little time as 30 min in basic environment with the aid of ultrasound irradiation without losing the integrity and stability of the pore structure of the final materials. The rapid formation of the mesostructure was attributed to the generation of localized hot spots at the surfactant–silicate interface caused by the application of ultrasonic irradiation, which accelerates the silica polymerization [32]. However, the ordered mesoporous structure was not observed after ultrasonic irradiation for 15min, which suggests that at least 30min were required for the formation of well-ordered MCM-41materials.

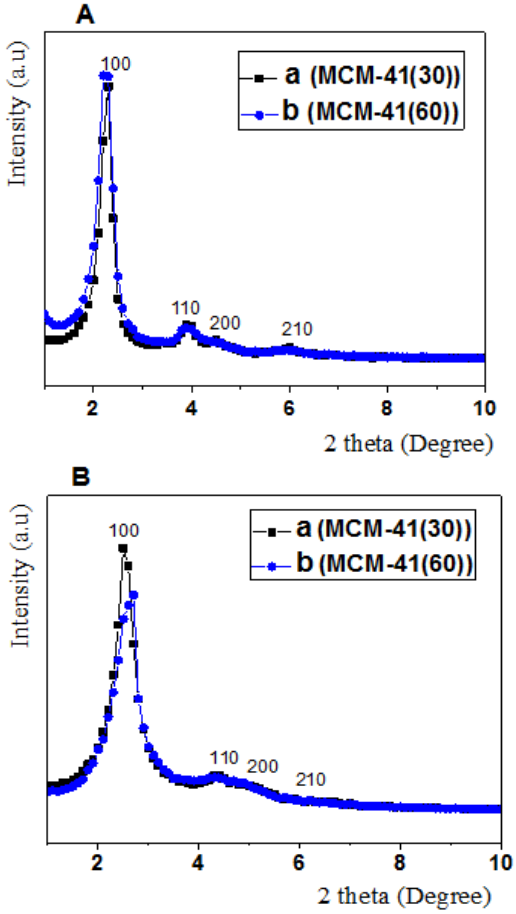

Fig. 4. Small angle X-ray diffraction patterns of MCM-41 synthesized with ultrasonic irradiation at different times:

a-30min b-60min. (A:as-prepared); (B: calcined)

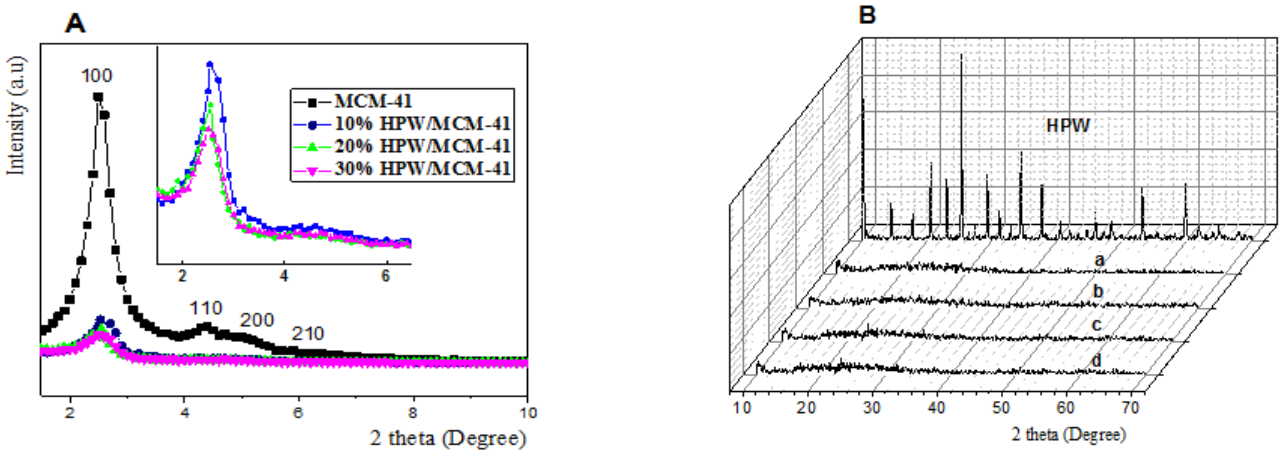

Fig. 5. (A) Low-angle XRD diffraction patterns of MCM-41 and HPW/MCM-41 samples. (B) High angle XRD diffraction patterns of pure HPW and HPW/MCM-41 samples: (a) MCM-41, (b) 10%HPW/MCM-41, (c) 20%HPW/MCM-41, (d) 30%HPW/MCM-41

Figure 5(A) displays the XRD patterns of calcined samples exposing the MCM-41 structure, before and after incorporation of different weight percentage of HPW, namely10, 20 and 30%. The (100) reflection of the MCM-41is still observed after HPW loading, although the diffraction peaks become broader and weaker as the HPW loadings increases up to 30%. This suggests that the mesoporous structure of the MCM-41 is preserved upon HPW loading, but the long-range order is significantly perturbed.

From the interplanar spacing of the basal reflection (d_{100}) it was possible to obtain the lattice parameter (a_0) for the hexagonal structure using the equation below [36]:

$$a_0 = \frac{2d_{100}}{\sqrt{3}}$$

were the value of a_o represents the sum of the pore diameter (D_{BJH}) and the silica wall-thickness (δ) :

$$a_0 = \delta + D_{BJH} \rightarrow \delta = a_0 - D_{BJH}$$

The structural and textural data allowed us to obtaining d_{100}, a_0 and δ values. These results are shown in table 1, indicating that impregnation of HPW caused significant modifications of the, and δ values and suggesting that HPW interacts with the inner MCM-41 pore surface. The δ values of the solids are 1.67 nm for the pristine MCM-41(30) and between 1.67 and 1.89 nm for HPW/MCM-41 catalysts, consistent with HPW localized on the inner pore surface and leading to a decrease in the pore diameter and an increased pore wall thickness, also suggesting good mechanical resistance. This assertion is consistent with previous reports indicating that solids with δ > 1nm have tetrahedra exposed at the pore surface, and thus, a good ability to withstand the load similar to macroscopic silica honeycombs with the same δ/a_0 ratio [37].

Although the presence of HPW usually decreases the long-range order of MCM-41[38, 39], there is less discussion to explain this phenomenon. Despite the significant alteration of the long-range order of the MCM-41 structure observed in the presence of HPW, the heteropolyacid crystal phase could not be detected in the samples, indicating that, although at relatively high concentrations, HPW is finely dispersed on the MCM-41 support, most likely filling the pores of the mesoporous material. The proposed model is consistent with the perturbation of the long range order of the MCM-41 observed for the HPW/MCM-41 materials, since some of the pore opening may be occluded by small HPW particles with maximum sizes in the range of the pore diameters. It also consistent with the significant decrease in the BET surface area and pore volume as the HPW loading increases from 0 to 30wt%. Since the pore diameter of our MCM-41 support is below 3 nm and our XRD instrument cannot detect crystallites below 3 nm in size, it is likely that most of the HPW dispersed on the surface is located inside the pores. If HPW crystallites were on the outer surface of the support, they would have been able to nucleate and form large crystals visible in XRD, at least for the highest HPW loading, but this is not the case.

TG/DTG analysis

The thermal stability of HPW and of the corresponding catalysts supported on MCM-41was investigated by TG/DTG analysis. TG/DTG analyses provide information about the stability of the samples with respect to the loss of weight due to physical and/or chemical transformations, i.e. loss of water or thermal decomposition. The catalytic activity and structure of the heteropolyacids mainly depend upon their degree of hydration. The results for bulk and supported HPW are displayed in figure 6. In agreement with previous reports [40, 41], the TGA curve of the bulk HPW shows a 7.5% weight loss within the temperature range from 70 to 120°C, which is associated with the loss of adsorbed water molecules. Further, it shows 3.5% weigh loss between 180 and 250°C, due to the loss of crystallization water, and 1-1.5% weigh loss at temperature higher than 420°C, attributed to the loss of constitutional water resulted from the decomposition of the Keggin anion (fig. 6(a). This thermal behavior observed for HPW is consistent with previous literature reports [41,42].

In the case of HPW supported on MCM-41, from the TGA thermal curves one can notice a slightly different

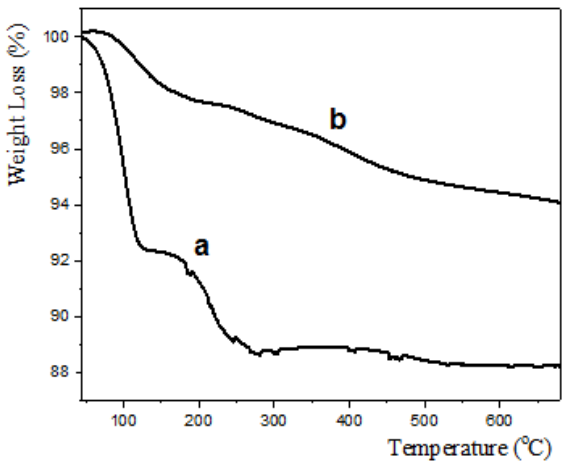

Fig. 6.TGA profile of pure HPW heteropolyacid(a) and 30%HPW/MCM-41(b)

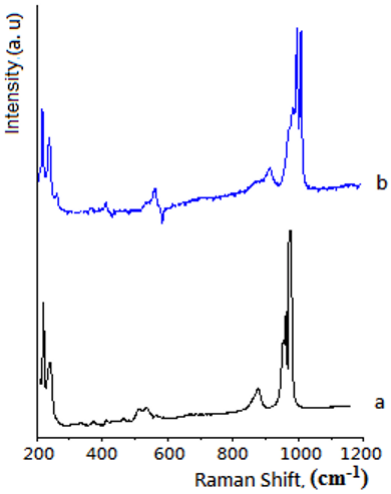

Fig. 7.The Raman spectra ofbulkHPW (a) and 30%HPW / MCM-41 (b)

behavior compared with the bulk HPW in the temperature range corresponding to the elimination of the adsorbed water (fig. 6b). The TGA of HPW/MCM-41 shows an initial weight loss of 2.5% at 90-150°C, significantly smaller compared to the 7.5% observed for the bulk material in the similar temperature range. We should note that there is no weight loss in the temperature range corresponding to desorption of crystallization water (i.e. 180-250°C), consistent with the absence of a crystalline HPW phase on the surface of our resulting catalysts observed from the XRD results, as discussed above. The second weight loss, consisting of 1.5% was observed at temperatures higher than 220°C, corresponding to the loss of the constitutional water of the Keggin ion. The relatively higher temperature values for the desorption of the constitutional water molecules of the Keggin anions are likely due to the difficulty in removal of water contained in HPW molecules inside channels of MCM-41. However, the interaction between the Keggin structures and the MCM-41 silica wall may also play an important role in the thermal stability of HPW particles at the surface, as well as the pore diameter of the MCM-41 support through a pore curvature effect that has been previously reported to have significant influence on the stability of metallic clusters dispersed on the MCM-41 surface [43]. These results are consistent with those previously reported [44, 45]. Generally, the thermal stability of heteropolyacids loaded on different supports depends on the type of the support, the HPW loading and the conditions of their pretreatment [46, 47].

Raman spectroscopy

The structural integrity of the Keggin unit was investigated by Raman spectroscopy, since the Kegging structures were very well characterized by this method [48].

The Raman spectra of HPW and 30%HPW/MCM-41 are shown in figure 7. We should mention that all HPW/MCM-41 samples showed similar Raman features, but with slightly different intensities. The Raman spectrum for bulk HPW shows bands at 1004, 991, 901, 544 and 215 cm^{-1}, which were assigned to symmetric (ν_s) and asymmetric (ν_{as}) vibrations of terminal oxygen ν_s(W-O_d), and ν_s(W-O_d), of corner shared bridged oxygen ν_{as}(W-O_b-W), of shared bridged oxygen ν_s(W-O-W), and of oxygen in central tetrahedron ν_s(P-O_a) [49, 50]. In the Raman spectra of HPW dispersed on MCM-41, the presence of the strongest characteristic bands ν_s(W-O_d)at 1004 cm^{-1}, ν_s(W-O_a)at 215cm^{-1} and ν_s(W-O_c-W) at 540cm^{-1} confirm the presence of Keggin anion at the surface. In case of the 30%HPW/MCM-41 catalyst, the absence of significant band shifts in the spectra indicates that the environment of the Keggin unit is similar to that of the bulk HPW, which suggests a rather weak interaction between the dispersed HPW and the MCM-41 support.

Conclusions

We have demonstrated that the ultrasonic synthesis of MCM-41 can reduce the synthesis time from days to a few minutes. Ultrasonic irradiation is an easy way to control the synthesis conditions, and most importantly, the structural properties of the MCM-41 materials can be finely adjusted by varying the synthesis time. XRD, nitrogen adsorption–desorption isotherms and Raman spectroscopy show that Keggin ion structure of HPW formed inside the pore surface of molecular sieve and is stable after anchoring to MCM-41. Raman investigations suggest a rather weak interaction between the Keggin structure of the HPA and the surface silanol groups of MCM-41; however, as water desorption from the HPW supported on MCM-41, corroborated with the XRD results indicated a crystalline HPW does not form at the surface, an important effect of the pore radius of curvature on the stability and catalytic activity of the MCM-41 supported Keggin structures cannot be ruled out.

Acknowledgements: This work has been financially supported by the doctoral program of the Romanian Ministry of National Education (No. 40784/CMJ/08.10. 2012). We also express our gratitude to Dr. Daniela Predoi from IFTM Magurele for her assistance and help with nitrogen adsorption isotherms.

References

1. KOZHEVNIKOV, I.V., Chemical Reviews, **98**, 1998, p. 171–198.
2. VOICU, V., BOLOCAN, I., CIUPARU, D., Rev. Chim. (Bucharest), **62**, no.12, 2011, p. 1206.
3. ZHU, K., HU, J.Z., SHE, X., LIU, J., NIE, Z., WANG, Y., PEDEN, C.H.F., KWAK, J.H., Journal of the American Chemical Society, **131**, 2009, p. 9715–9721.
4.VOICU, V., BOMBOS, D., BOLOCAN, I., JANG, C.R., CIUPARU, D., Rev. Chim. (Bucharest), **63**, no.2, 2012, p. 200.
5. YANG, X. K., CHEN, L. F., WANG, J. A., NORENA, L. E., Catalysis Today, **148**, 2009, p. 160–168.
6. KRESGE, C. T., LEONOWICZ, M. E., ROTH, W. J., VARTULI, J. C., BECK, J. S., Nature, **359**, 1992, p. 710-712.
7. BECK, J. S., VARTULI, J. C., ROTH, W. J., LEONOWICZ, M. E., KRESGE, C. T., Journal of the American Chemical Society, **114**, 1992, p. 10834-10843.
8. JANG, C.R., MATEI, V., VOICU, V., BORCEA, A., CIUPARU, D., Rev. Chim. (Bucharest), **65**, no.12, 2014, p. 1525.
9. LUCHIAN, C., NICULAUA, M., COTEA, V. V., BILBA, N., COPCIA, V., SANDU, A.V., Rev. Chim. (Bucharest), **62**, no.3, 2011, p. 287.
10. AMAMA, P. B., LIM, S., CIUPARU, D., PFEFFERLE, L., HALLER, G. L., Microporous and Mesoporous Materials, **81**, 2005, p. 191-200.
11. GHITA, D., ROSCA, P., STANICA EZEANU D., Rev. Chim. (Bucharest), **63**, no.10, 2012, p. 1056.
12. NEDUMARAN, D., PANDURANGAN, A., Materials Research Bulletin, **61**, 2015, p. 1-8.
13. CAI, C., WANG, H., HAN, J.Y., Applied Surface Science, **257**, 2011, p. 9802-9808.
14. KOZLOVA, S. A., KIRIK, S. D., Microporous and Mesoporous Materials, **133**, 2010, p. 124-133.
15. RUSSO, P. A., RIBEIRO CARROTT, M. M. L., CARROTT, P. J. M., Colloids and surfaces A: Physicochemical Enginnering Aspects, **310**, 2007, p. 9-19.
16. ROIK, N. V., BELYAKOVA, L. A., Journal of Solid State Chemistry, **207**, 2013, p. 194-202.
17. SCHILLER, R., WEISS, C.K., GESERICK, J., HUSING, N., LANDFESTER, K., Chemistry of Materials, **21**, 2009, p. 5088–5098.

18. VOEGTIN, A. C., MATIJASIC, A., PATARIN, J., SAUERLAND, C., Microporous Materials, **10**, 1997, p. 137-147.
19. MELENDEZ-QRTIZ, H. I., GARCIA-CERDA, L. A., QLIVARES-MALDONADO, Y., Ceramics International, **38,** 2012, p. 6353-6358.
20. TANG, X., LIU, S., WANG, Y., HUANG, W., SOMINSKI, E., PALCHIK, O., KOLTYPIN, Y., GEDANKEN, A., Chemical Communications, 2000, p. 2119–2120.
21. NEWALKAR, B. L., KOMARNENI, S., KATSUKI, H., Chemical Communications, 2000, p. 2389.
22. BANG, J. H., SUSLICK, K. S., Advanced Materials, **22**, 2010, p. 1039–1059.
23. LI, H., HAN, C., Chemical of Materials, **20**, 2008, p. 6053–6059.
24. WEN, P., TIE, W., WANG, L., LEE, M. H., LI, X. D., Materials Chemical and Physics, **117**, 2009, p. 1–3.
25. GEDANKEN, A., Current Science, **85,** 2003, p. 1720.
26. HANU, A. M., POPOVICI, E., COOL, P., VANSANT, E. F., Studies in Surface Science and Catalysis, **165**, 2007, p. 169-172.
27. LIM, S., YANG, Y. H., CIUPARU, D., WANG, C., CHEN, Y., PFEFFERLE, L., HALLER, G. L., Topics in Catalysis, **34**, 2005, p. 31-40.
28. RUN, M., WU, S., WU, G., Microporous and Mesoporous Materials, **74**, 2004, p. 37–47.
29. VTRIVEL, S., CHEN, C.T., KAO, H. M., New Journal of Chemistry, **34,** 2010, p. 2109-2112.
30. PALANI, A., WU, H.Y., TING, C. C., VETRIVEL, S., Microporous and Mesoporous Materials, **131**, 2010, p. 385.
31. LEE, S. K., LEE, J., JOO, J., HYEON, T., AHN, W. S., LEE, H., LEE, C., CHOI, W., Journal of Industrial and Engineering Chemistry, **9**, 2003, p. 83.
32. GEDANKEN, A., TANG, X., WANG, Y., PERKAS, N., KOLPYPIN, Y., LANDAU, M.V., VRADMAN, L., HERSKOWITZ, M., Chemistry European Journal, **7**, 2001, p. 4546–4552.
33. SIAHKALI, A. G., PHILIPPOU, A., DWYER, J, ANDESON, M. W., Applied Catalysis A: General, **192**, 2000, p. 57–69.
34. MENDEZ, F. J., LLANOS, A., ECHEVERRIA, M., JAUREGUI, R., VILLASANA, Y., Fuel, **110**, 2013, p. 249-258.
35. SRIVASTAVA, D. N., PERKAS, N., ZABAN, A., GEDANKEN, A., Pure and Applied Chemistry, **74**, 2002, p. 1509–1517.
36. SOUZA, M. J. B., ARAUJO, A. S., PEDROSA, A. M. G., MARINKOVIC, B. A., Materials Letters, **60**, 2006, p. 2682–2685.
37. DESPLANTIER-GISCARD, D., GALARNEAU, A., DI RENZO, F., FAJULA, F., Materials Science and Engineering: C, **23**, 2003, p. 727–732.
38. JERMY, B. R., PANDURANGAN, A., Applied Catalysis A: General, **295**, 2005, p. 185–192.
39. CAI, Q., LUO, Z. S., PANG, W. Q., FAN, Y. W., CHEN, X. H., CUI, F. Z., Chemistry of Materials, **13**, 2001, p. 258.
40. DEGIRMENCI, L., OKTAR, N., DOGU, G., Fuel Processing Technology, **91**, 2010, p. 737-742.
41. KHDER, A. E. R. S., HASSAN, H. M. A., EL-SHELL, M. S., Applied Catalysis A: General, **411-412**, 2012, p. 77-86.
42. BIELANSKI, A., LUBANSKA, A., Journal of Molecular Catalysis A: Chemical, **224,** 2004, p. 179–187.
43. LIM, S., CIUPARU, D., CHEN, Y., YANG, Y., PFEFFERLE, L., HALLER, G. L., Journal of Physics Chemistry B, **109,** 2005, p. 2285-2294.
44. KAMALAKAR, G., KOMURA, K., KUBOTA, Y., SUGI, Y., Journal of Chemical Technology and Biotechnology, **81**, 2006, p. 981.
45. BRAHMKHATRI, V., PATEL, A., Industrial and Engineering Chemistry Research, **50**, 2011, p. 13693–13702.
46. LLANOS, A., MELO, L., AVENDANO, F., MONTES, A., BRITO, J. L., Catalysis Today, **133-135**, 2008, p. 20-27.
47. YUAN, C., CHEN, J., Chinese Journal of catalysis, **32**, 2011, p. 1191-1198.
48. POPA, A., SASCA, V., KISS, E. E., MARINKOVIC-NEDUCIN, R., Materials Research Bulletin, **46**, 2011, p. 19-25.
49. ROCCHICCIOLI-DELTCHEFF, C., FOURNIER, M., FRANK, R., THOUVENOT, R., Inorganic Chemistry, **22**, 1983, p. 207.
50. BRIDGEMAN, A., Chemical Physics, **287**, 2003, p. 55.

Manuscript received: 29.07.2016